Optical emission spectroscopy study on flashover along insulator surface due to particle contamination

SOMESH VINAYAK TEWARI,[1] R.J. KSHIRSAGAR,[2] AMITAVA ROY,[1] R. SARATHI,[3]
ARCHANA SHARMA,[1] AND K.C. MITTAL[1]

[1]Accelerator and Pulse Power Division, Bhabha Atomic Research Centre, Trombay, Mumbai, India
[2]High Pressure and Synchrotron Radiation Physics Division, Bhabha Atomic Research Centre, Trombay, Mumbai, India
[3]Department of Electrical Engineering, Indian Institute of Technology, Madras, Chennai, India

Abstract

The surface flashover behavior in ambient air and nitrogen are studied at a pressure of $1 \, \mathrm{kg/cm^2}$ using optical emission spectroscopy. A high dc voltage is applied to Rogowski profile electrodes with polyoxymethylene as the insulator between the electrodes. Three different conditions of needle protrusion along the surface of polyoxymethylene are used to study the variation in spectral characteristics due to particle contamination. When the insulator is placed between the spark gap electrodes, the OES spectra are dominated by the H_α line in air and nitrogen medium. It was found that the intensity of N_2^+ (B-X) emission is less in air surrounding the insulator medium. The plasma temperature during bulk breakdown in air is 0.433 eV, which increases to 0.434 eV with the pressurized nitrogen, which further increases in the presence of insulator to 0.441 eV and 0.44 eV in nitrogen and air, respectively. The electron density is obtained from the N emission line at 746.8 nm and the estimated peak value is $2.85 \times 10^{12} \, \mathrm{cm^{-3}}$ in the presence of insulator. The plasma temperature decreases with increase in distance of particle contamination from cathode. The increase in electron density in air, as compared to nitrogen implies more material desorption in air which is also supported by the comparisons of H_α lines.

Keywords: Optical emission spectroscopy; spark gap; insulator; surface flash over

INTRODUCTION

Spacers are used as solid insulating support for high voltage conductors in a compressed gas insulated system systems (GIS) (Laghari, 1985). These systems are subjected to very fast transient over voltages (VFTO), which lead to their insulation failure due to flashover along insulator surface. This involves the formation of discharge path along the surface of the insulator that leads to breakdown at a reduced voltage. The presence of spacer between spark gap electrodes is necessary in the study of operation of GIS under VFTO especially when a series of breakdown occurs during the working of a disconnector (Ran *et al.*, 2013). The spacer plays a critical role in Blumlein pulse forming line (PFL) based high voltage pulse power systems. Blumlein consists of two PFL, one between the outer and intermediate conductor and the other between the inner and intermediate conductor (Roy *et al.*, 2008; Kumar *et al.*, 2007). However, it consists of support insulators between these conductors the design

of which is of considerable importance for reliable operation at high voltages. Further the energy mismatch between Marx generator and Blumlein leads to the development of high field stresses followed by failure of the solid support insulation (Sharma *et al.*, 2014). The discharge along insulator surface in compressed gases involves a number of electron-photon processes in the surrounding gas volume that modifies the ionization parameters which influences the ionization growth (Sudarshan *et al.*, 1986). The presence of spacer in compressed gases significantly reduces the breakdown voltage and increases the speed of propagation of electrons between the electrodes (Li *et al.*, 1995a). The discharge can initiate at any point on the surface of the spacer (Pfeiffer, 1982) and the high speed photographic study shows a consistent growth of charge carriers along the spacer surface which helps in discharge development (Li *et al.*, 1995b). Time-resolved optical and electrical study of the avalanche and streamer formation in uniform fields without space charge effects have already been carried out in nitrogen and air (Kennedy, 1995; Wen, 1989; Verhaart, 1982). A number of studies have been carried out in recent times to study the development of arc and flashover along an ice covered

Address correspondence and reprint requests to: Somesh Vinayak Tewari, Accelerator and Pulse Power Division, Bhabha Atomic Research Centre, Trombay, Mumbai, India. E-mail: somesh_vinayak@yahoo.com

insulator using optical emission spectroscopy (OES) to study the different plasma parameters and the contribution of different particles in the plasma processes (Nekahi *et al.*, 2014; 2011*a*). The method of OES is passive and is based on recording light emitted from the plasma. The collision with electrons leads to excitation of plasma particles. The relaxation of the excited particles to lower energy state is the reason of emission of photon of light (Kolpaková *et al.*, 2011). The ablation of materials by electrical spark plasma forms the basis of analysis of OES. The excited ablated material in the plasma emits light in the vacuum ultraviolet (UV) to visible range, the wavelength of which is the characteristic of the element present in the sample and its intensity is a measure of its concentration. The ablation of zinc-oxide films caused by yttrium garnet aluminum (Nd:YAG) laser was studied using OES and it was observed that the electron temperature and densities decreases with distance from the target being 1.2 eV and 3.2×10^{17} cm^{-3}, respectively, with a small rise at a distance of 20 mm from the target (Saji *et al.*, 2006). The spectroscopic studies on plasma produced from a laser ablated magnesium-sulphate surface shows a reduction in temperature and electron density for both the incident laser wavelengths of 1064 nm and 532 nm (Salik *et al.*, 2014). The enhancement in emission from lithium at 670.8 nm as compared to the transition at 610.3 nm in the presence of a variable magnetic field shows electron impact excitation as the dominant mechanism behind the increase in intensity line at 670.8 nm as compared to recombination (Kumar *et al.*, 2010). Time and space resolved spectroscopic study of discharge in pure helium gas environment at a pressure of 10^5 Pa shows the formation of discharge channel within the gap with varying plasma densities comprising of an inner high dense layer of the order 3×10^{16} cm^{-3} and an outer lower density layer of 5×10^{15} cm^{-3} with temperature of these layers being 2 eV (Yatom *et al.*, 2013). The layering of the plasma at the gas plasma interface into fast and slow ion components with fast component penetrating into the ambient gas and deceleration of the slow component gives a double peak in the temporal profile of laser produced carbon plasma (Thareja *et al.*, 1995). OES was carried out for the determination of the excitation temperature of an arc over an ice covered insulator surface (Nekahi & Farzaneh, 2011*b*). The excitation temperature was determined using relative line intensity method by using the copper and oxygen spectral line, which was found to be 9000 K and it did not vary significantly with the discharge current (Nekahi & Farzaneh, 2011*b*). The OES of dc flashover along lexan surface in air and nitrogen shows that the discharges propagates close to the surface in air and away from it in pressurized nitrogen (Krile *et al.*, 2004). The pulsed flashover of lexan in nitrogen environment leads to the development of flashover path along the insulator surface in the presence of UV illumination and away from the surface in the absence of UV. This is due to the presence of photo-electrons, which helps in spark development close to the insulator surface. A decrease in flashover delay time in humid nitrogen is due to the presence of

weakly bound electrons in moisture which is available for flashover initiation (Morales *et al.*, 2006; Krile *et al.*, 2008; 2005). However, in the absence of UV, the flashover path in air is close to the insulator surface and away from it in nitrogen environment mainly due to the presence of oxygen in air, which has a lower excitation threshold leading to larger production of photoelectrons close to the insulator (Morales *et al.*, 2007). The streamer propagation study of magnesium-fluoride in nitrogen, oxygen, and dry air using an intensified charge-coupled device camera shows streamer initiation at anode which is segmented in nitrogen environment unlike in oxygen where the streamer growth is blurry and diffused with self-absorption of emission lines by oxygen molecules in vacuum UV range (Laity *et al.*, 2011). The presence of needle protrusion at 1 mm above the insulator surface leads to the formation of discharge path in gas away from the insulator surface similar to the plain gas gap conditions with perturbation, which signifies the importance of the region of highest stress in determining the discharge initiation and propagation particularly for fast voltage transients (Pfeiffer *et al.*, 1980). The presence of particle on spacer surface provides a local field enhancement and the phenomenon of breakdown was modeled by considering avalanche growth in the surrounding of the particle (Cooke, 1982). The objective of this paper is to study the effect of particle contamination (needle protrusion) on spectral characteristics of discharge along insulator surface. It provides an insight into the variation of plasma parameters (plasma temperature and electron density) with distance of particle from cathode. A comparison of H$_\alpha$ line in an insulator bridged gap in air and nitrogen medium is carried out by using the line broadening of H$_\alpha$.

EXPERIMENTAL METHODS

The experimental setup for the OES studies on the insulator surface is shown in Figure 1. A single phase ac supply is fed to a step up transformer arrangement with a secondary voltage of 100 kV. The output of the step-up transformer is fed to a voltage-doubter circuit for the generation of a high voltage dc output which is fed to the spark gap electrodes enclosed within a Perspex chamber for high pressure studies. The spark gap chamber has a view port arrangement of diameter 150 mm where the lens arrangement is placed perpendicular to path of spark gap discharge to capture the light generated as a result of gap breakdown. Two Rogowski profile electrodes of 90 mm diameter and 36 mm thickness forms the spark gap electrodes with a cylindrical spacer of 36 mm diameter and 20 mm thickness placed in between the two electrodes. The spacer used is polyoxymethylene commercially known as delrin, which is a commonly used insulator in pulse power systems. The configuration of spark gap electrodes along with the spacer arrangement is very similar to the configurations reported in the literatures for surface flashover study (Ran *et al.*, 2013; Ping Yan *et al.*, 2011). Table 1 gives the characteristics of the insulating material used between the electrodes.
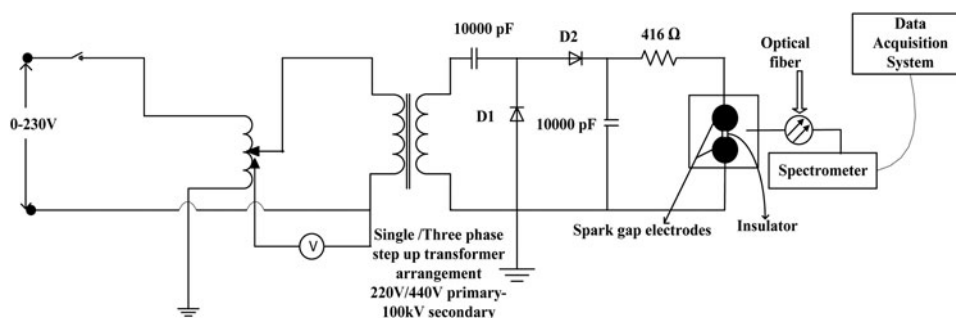
Fig. 1. Equivalent circuit of the high voltage dc generation and optical spectroscopy measurement

OES is used to determine the spectrum of the plasma with the collected light mainly coming from the bulk of the plasma. However, there could be some emissions from regions near the electrodes. The emissions produced as a result of surface discharge in air and nitrogen is collected using a 150 mm focal length lens and is coupled to a time integrated spectrometer (Ocean Optics, USB 2000) using a multimode optical fiber arrangement with a core diameter of 400 μm. The integration time of the spectrometer is 1 ms to 65 s, baseline corrected wavelength value of 750 nm and the optical fiber used for signal capture subtends an acceptance angle of 25.4° with a solid angle of 1.491sr. A positive dc voltage of 50 kV was applied to the cylindrical samples of polyoxymethylene with the samples prepared in the following configuration as shown in Figure 2: (1) Needle of 3 mm length with a diameter of 1 mm connected at the cathode tip of the insulator (Type I). (2) Needle of 3 mm length with a diameter of 1 mm connected at the center on the surface of the insulator (Type II). (3) Needle of 3 mm length with a diameter of 1 mm connected at the anode tip of the insulator (Type III). The intensity lines were studied with the three sample configurations in air and nitrogen compressed at a pressure of 1 kg/cm^2 to analyze the effect of location of particle contamination on the flashover path.

RESULTS AND ANALYSIS

Analysis of Surface Flashover Activity in Air Ambience by OES

The phenomenon of surface flashover is analyzed based on the relative intensity of the constituents present in the

Table 1. *Characteristics of sample (polyoxymethylene)*

Dielectric strength	19.68 kV/mm
Dielectric constant (relative to air)	3.7
Loss tangent	0.0085@0.5 MHz
Surface roughness	p360
Composition (Chemical formula)	$(CH_2O)_n$

emission spectra during the discharge phase. However, emphasis is laid on the study of the variations in the emission spectra as a result of the introduction of particle contamination at different positions along insulator surface. The need of needle protrusion along the surface of the insulator creates field non-uniformity and initiates discharge along a particular path. Each spectral data is an average of five shots. The emission spectra profile of a spark gap discharge with air as the background medium in the absence of an insulator is shown in Figure 3. A high intensity count of singly ionized nitrogen is observed in emission spectra of air. The spectra clearly shows a part of the molecular band emission spectrum of N_2 (C-B) second positive system, which covers a range 300–450 nm and N_2 (B-A) first positive system in the range 600–850 nm. The N_2^+ (B-X) first negative system has a spectral band at 391 nm is present in the emission spectra but is not very prominent. Other lines observed in the spectra originate from excited N and N^+ species (Horst *et al*., 2012). Air has nitrogen in maximum composition which leads to the highest intensity of N^+ in the emission spectra at 500.5 nm and 656 nm as compared to other excited constituents like N and N^+ species. The line at 777 nm is of resonant O I as both nitrogen and oxygen form the major constituents of air. The different spectral lines are identified with the use of Lofthus *et al*. (1977) and the NIST database (Ralchenko *et al*., 2013). The experiment is repeated with an insulator placed between the two electrodes. A needle protrusion as shown in Figure 2 is placed at cathode and the emission spectra are observed in Figure 4. The spectra shows an increase in the intensity of hydrogen (H_α) at 656.3 nm (Bruggeman *et al*., 2009) unlike in air which signifies the fact that discharge takes place along insulator surface in a gas insulated system bridged by a solid dielectric. However, the peak observed near 656 nm is that of N^+ (Horst *et al.*, 2012) on which H_α is superimposed leading to an increase in intensity at 656.3 nm in the presence of an insulator.

Figures 5 and 6 shows the emission spectra of spark gap discharge when needle is placed at the center and at the anode end along the surface of the insulator, respectively. The maximum intensity of H_α line is observed when needle electrode is placed at the center. This implies that placing a needle at the center reduces the effective gas gap. Discharge paths are formed between the needle and both
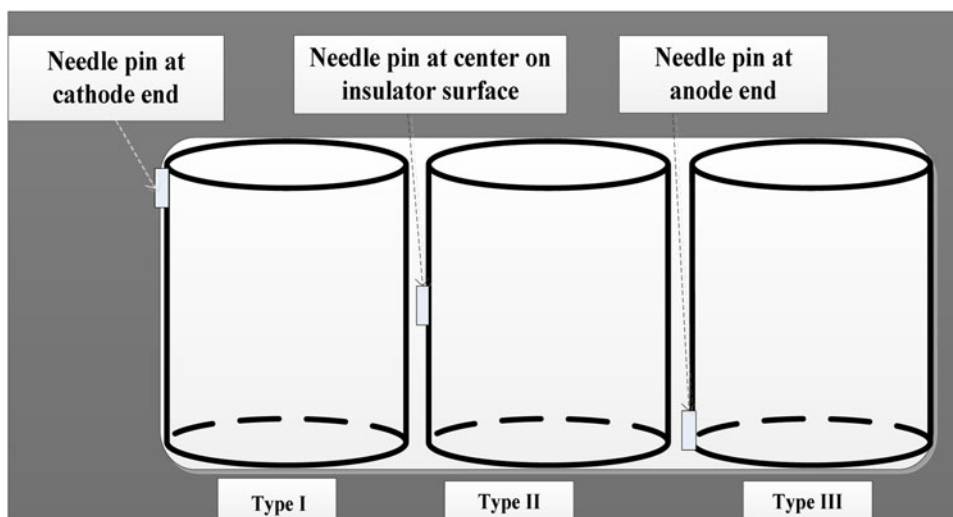
Fig. 2. Sketch of different types of sample used.

the electrodes in either direction, leading to greater removal of the materials from insulator surface, which in turn leads to highest intensity of H_α in the atomic spectral lines. With needle protrusion placed at the anode end, however, comparable intensities of nitrogen N^+ and H_α lines are observed in the atomic spectra. This explains the fact that the spark bifurcates and multichannel discharge takes place both in the gas and along the surface of the insulator leading to nearly same intensities of both the elements.

Analysis of Surface Flashover Activity in Nitrogen Ambience by OES

The experiments are repeated to optically study the discharge in nitrogen at a pressure of 1 kg/cm^2 as the background gas instead of air. Figure 7 shows the spectral lines of spark gap discharge in compressed nitrogen gas. A slight reduction in

the values of intensities of singly ionized nitrogen is obtained, which signifies suppression in the intensity of spark discharge in compressed gases. The spectra show a peak in the range of 391 nm which is a molecular band spectrum of N_2^+ (B-X) first negative system clearly visible in the spectrum. The spark gap breakdown consists of mainly the ignition and spark phase. The line band around 568 nm is that of N^+, which implies that there is no significant molecular emission during the spark phase and the emission of first positive system in the spark phase is mainly because of the overlap between the N_2 (B-A) and atomic nitrogen lines (Horst *et al.*, 2012). Similarly the peak around 525 nm is that of presence of atomic nitrogen in the spark phase of discharge. However, in the presence of an insulator, the lines at 568 nm and 525 nm are suppressed as shown in Figures 8, 9, and 10. This shows that the H_α line plays the major role at 656.3 nm which suggest that discharge takes place along
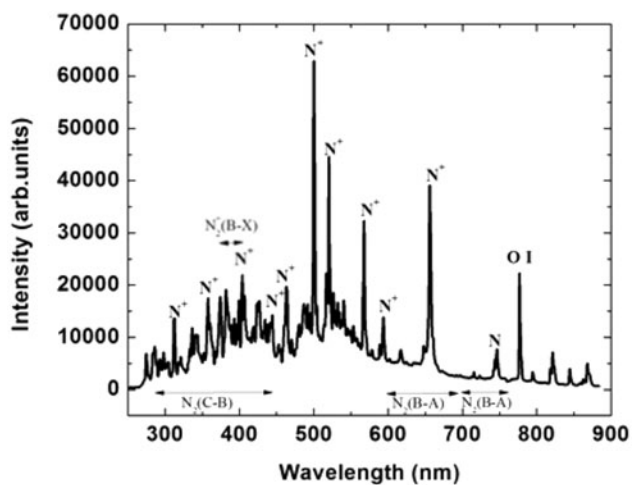

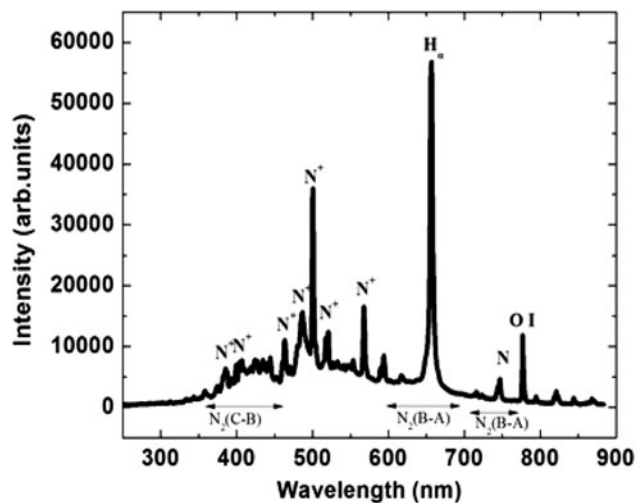**Fig. 3.** Optical emission spectra of spark gap discharge in air.

Fig. 4. Optical emission spectra of spark gap discharge in air along insulator surface when needle protrusion is at the cathode.
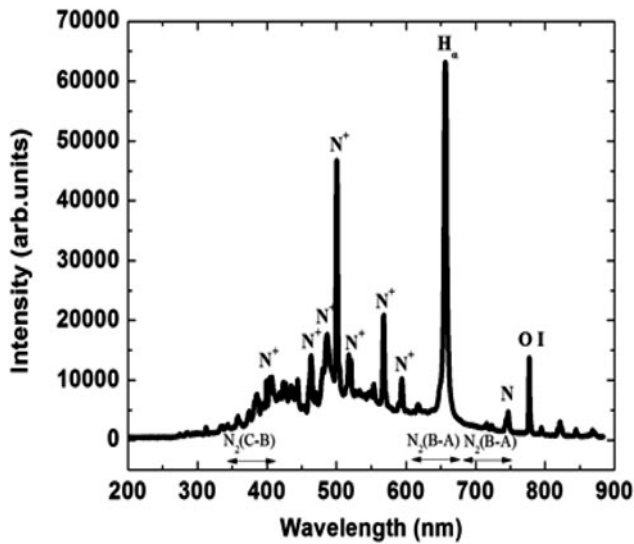
Fig. 5. Optical emission spectra of spark gap discharge in air along insulator surface when needle protrusion is at the center.

Fig. 7. Optical emission spectra of spark gap discharge in nitrogen.

which oxygen is 20% by volume which contributes to the high intensity value of O I line.

Comparison of H_α in Air and Nitrogen Medium

The effect of needle protrusions at different points along the insulator surface is analyzed on the basis of line broadening of H_α in nitrogen and air with insulator. The measured H_α intensity is fitted with a Lorentzian line shape. The full width at half maximums (FWHMs) is then estimated from the fitted curve. The discharge initiates at the triple point (cathode + insulator + gas) and arc begins to develop close to the surface leading to slight ionization and arc development. The FWHM estimated from the H_α line broadening are (3.90 ± 0.06) nm and (3.327 + 0.12) nm in air and nitrogen, respectively. When the needle is placed at the center along the insulator surface there is further increase in ionization and expansion of arc leading to increase in FWHM. Maximum

the insulator surface. When the needle is present at the anode end of the insulator, the discharge phenomenon is very similar to the one taking place in the air medium with needle at anode. The emission in the ignition phase of discharge mainly comes from the first positive system, second positive system, and first negative system of nitrogen (Horst *et al.*, 2012).

In the presence of insulator, these band intensities are drastically reduced due to a decrease in voltage withstand strength and emission takes place from any point on the surface of the insulator. The nitrogen used in the flashover study is an IOLAR grade with two percent oxygen as impurity. This results in the presence of a resonant O I at 777 nm. However, the intensity value is very less when compared to flashover along the insulator surface in ambient air medium in
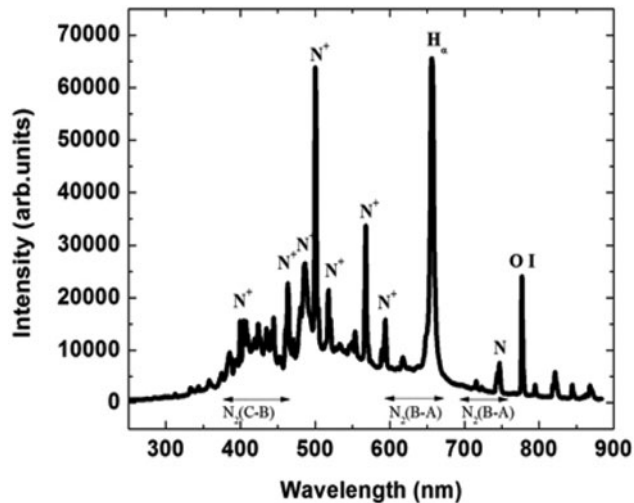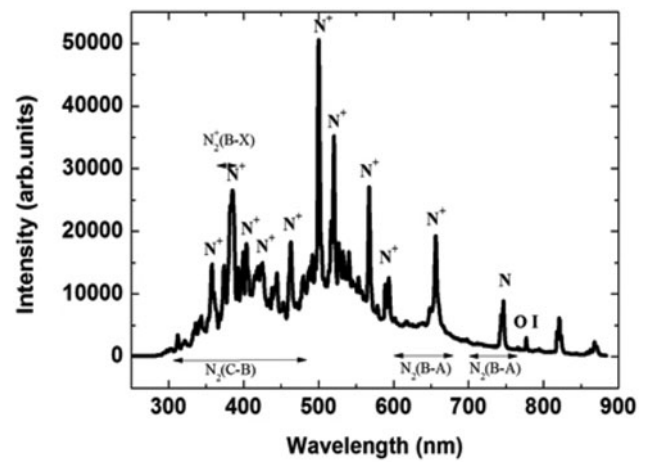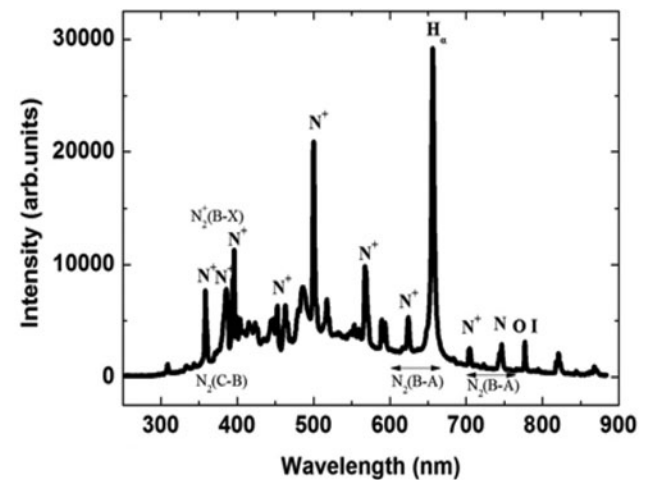

Fig. 6. Optical emission spectra of spark gap discharge in air along insulator surface when needle protrusion is at the anode.

Fig. 8. Optical emission spectra of spark gap discharge in nitrogen along insulator surface when needle protrusion is at the cathode.
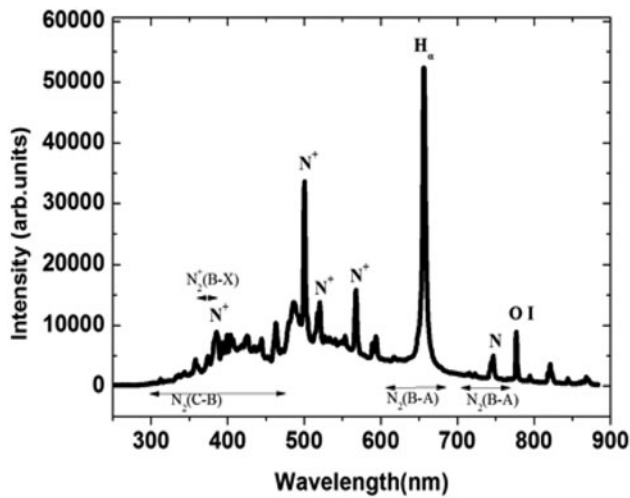
Fig. 9. Optical emission spectra of spark gap discharge in nitrogen along insulator surface when needle protrusion is at the center.

Fig. 11. Line broadening of H_α in nitrogen and air with insulator (needle at anode).The spectrum of N is subtracted from the spectrum of H_α and N to obtain only the H_α line.

value of FWHM is observed when the needle is at anode, where the arc has completely expanded leading to maximum line intensity. This suggests that the Doppler broadening of the lines to be dominant. Figure 11 shows line broadening of H_α in air and nitrogen with needle (protrusion) at anode.

Table 2 shows a comparison of FWHM in air and nitrogen for different positions of the needle protrusions. The continuous increase in FWHM in air as the protrusion moves away from the cathode is mainly due to the presence of moisture in air. The hydrogen present in moist air ionizes more rapidly than the ionization of hydrogen along the insulator surface. However, such freely available hydrogen is not present in a pure nitrogen environment which leads to an increased value of intensity and hence an increased FWHM in air than in nitrogen.
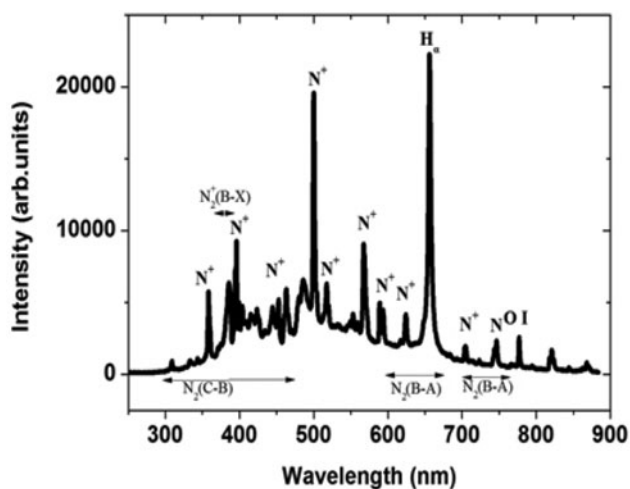
Estimation of Plasma Temperature and Electron Density

The variation in plasma temperature and electron density is studied as a function of distance of the particle protrusion from the cathode along the surface of the insulator. The line pair approach was used to estimate plasma temperature and density in which relative intensities of emission lines were used. The plasma temperature and density estimations are based on the assumption of local thermodynamic equilibrium (Antony *et al.*, 2010). For the plasma in local thermodynamic equilibrium, the energy level population of the different species is given by the Boltzmann's law (Unnikrishnan *et al.*, 2010)

$$\frac{n_{a,z}}{n_z} = \frac{g_{a,z}}{P_z} \exp\left(\frac{-E_a Z}{K_B T}\right), \tag{1}$$

Z refers to the ionization stage of the species ($Z = 0$ and 1 correspond to neutral and single ionized atoms, respectively) k_B is the Boltzmann's constant, T is the plasma temperature, $n_{a,z}$, E_a and $g_{a,z}$ are the population, energy, and degeneracy of the upper energy level a, n_z is the number density and P_z is partition function of the species in ionization stage Z. The integrated intensity I_z of a spectral line occurring between

Fig. 10. Optical emission spectra of spark gap discharge in nitrogen along insulator surface when needle protrusion is at the anode.
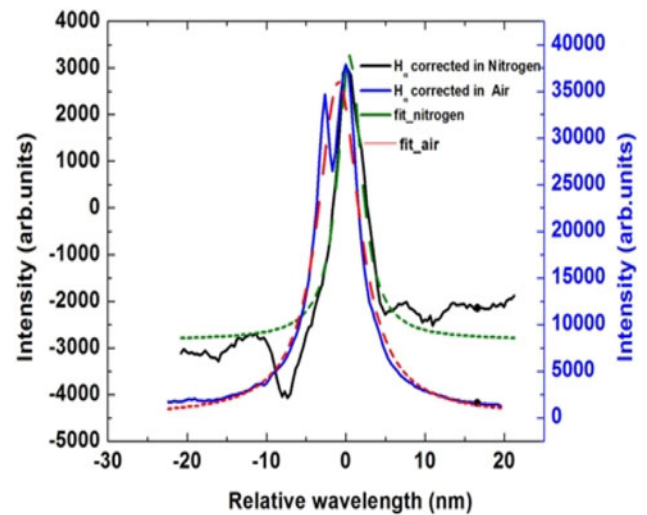
Table 2. *Shows a comparison of FWHM in air and nitrogen for different positions of the needle protrusions*

Needle position	Air	Nitrogen
At cathode	(3.90 $\pm$ 0.06) nm	(3.32 $\pm$ 0.12)nm
At centre	(4.32 $\pm$ 0.05) nm	(4.32 $\pm$ 0.05)nm
At anode	(6.44 $\pm$ 0.22) nm	(3.37 $\pm$ 0.02)nm

upper and lower energy level i of the species in the ionization stage Z is given by

$$I_z = \frac{hc}{4\Pi\lambda_{ai,Z}} A_{ai,Z} \frac{n_{a,z}}{P_z} g_{a,z} L \exp\left(\frac{-E_{k,z}}{K_B T}\right), \qquad (2)$$

where h is the Planck's constant, c is the speed of light, L is characteristics length of plasma, $\lambda_{ai,Z}$ is the transition line wavelength and $A_{ai,Z}$ is the transition probability.

The intensity ratio of the two lines of the same species of the ionization stage Z is given by

$$\frac{I_1}{I_2} = \frac{\dfrac{hc}{4\Pi\lambda_{ki}} A_{ki,Z} g_{k,z} L \exp\left(\dfrac{-E_{1,z}}{K_B T}\right)}{\dfrac{hc}{4\Pi\lambda_{nm}} A_{nm,Z} g_{n,z} L \exp\left(\dfrac{-E_{2,z}}{K_B T}\right)}, \qquad (3)$$

where I_1 is the line intensity from k-i is transition and I_2 is the line intensity from n-m transition.

Using Eq. (3) we have

$$T = \frac{(E_2 - E_1)}{K_B \ln\left(\dfrac{\lambda_{ki} A_{nm,z} I_1 g_{n,z}}{\lambda_{nm} A_{ki,z} I_2 g_{k,z}}\right)}. \qquad (4)$$

The wavelengths λ_{nm} and λ_{ki} of N^+ lines used in the temperature calculation are 567.4 nm and 500.5 nm, respectively. Figure 12 shows a variation of plasma temperature with distance of needle from cathode along the insulator surface. However, there is not much variation in temperature with distance of particle contamination from cathode. A slight increase in plasma temperature in nitrogen as compared to air can be attributed to reduction in the mean free path in nitrogen with pressure which leads to more number of collisions between the particles leading to an increase in temperature.
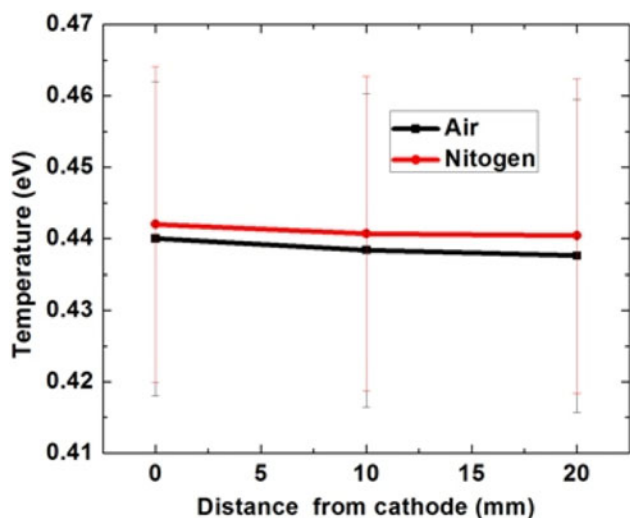
The ratio of the intensities which is evaluated using two similar wavelengths of nitrogen or air increases implying more ionization as observed with an increase in electron density as shown in Figure 13. This increased intensity ratio leads to reduction in plasma temperature as the particle moves away from the cathode. The effect is independent of the nature of the gas medium surrounding the particle. The results are similar to the study on laser produced carbon plasma in which the temperature shows a decreasing behavior with distance (Harilal *et al*., 1997). The electron density calculated from the atom and ion spectral lines that is emitted from the plasma produced by the discharge between the cathode anode (AK) gap is determined by the Saha-Boltzmann's equation and is given by

$$n_e = \frac{I_a}{I_i} 6.6 \times 10^{21} \frac{A_i g_i}{A_a g_a} \exp\left(\frac{E_{ion} + E_i - E_a}{T}\right), \qquad (5)$$

where n_e is the electron density, I_a and I_i are the intensity values of same species in different ionization stages, i.e., of N and N^+, E_i, $A_i g_i$, and E_a, $A_a g_a$ are the energy, transition probabilities of states and degeneracy of the upper energy level and E_{ion} is the minimum energy required to create an ion pair, respectively, obtained from the NIST database (Ralchenko *et al*., 2013). The wave-lengths of N^+ and N used in the density calculation are 500.5 nm and 746.8 nm, respectively. Figure 13 shows the variation in electron density with the distance of particle (needle) from cathode. An increase in the distance of particle away from cathode serves as conducting medium along the insulator surface which leads to more desorption of materials along the surface. Also the cumulative effect of secondary electron multiplication along the insulator surface lead to net increase in electron density as the particle moves away from the cathode. However, the density growth in nitrogen is less compared
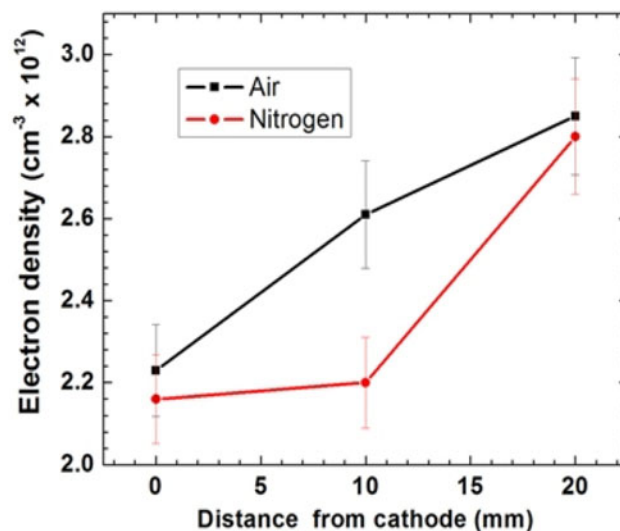

Fig. 12. Variation of plasma temperature with distance of needle from cathode.

Fig. 13. Variation of electron density with distance of needle from cathode.

to that in air proves the fact of higher breakdown voltage in nitrogen insulated gap. The additional electrons generated in the gap helps in rapid ionization of the gap causing the breakdown at a reduced voltage.

CONCLUSION

The technique of optical emission spectroscopy is used to study the dc discharge along polyoxymethylene subjected to particle contamination in air and nitrogen medium. A variation in the intensities of the constituent atoms implies material erosion and electron desorption from insulator surface which is being dependent on the position of the particle contamination along the insulator surface. A reduction in the intensity of spark is observed in nitrogen medium could be due to the reduction in energy gained between successive collisions as the pressure is increased and hence the collective intensity is less when the excited atoms return to the ground state.

A reduction is observed in the value of plasma temperature from 0.441 eV to 0.437 eV with increase in the distance of particle contamination from cathode. The increase in electron density from 2.1×10^{12} cm^{-3} to 2.8×10^{12} cm^{-3} can be attributed to increased material desorption and secondary electron multiplication with increase in distance of particle from cathode. Future work involves the use of different gases like argon, helium and different insulator materials to further study the variations in the discharge phenomena.

REFERENCES

ANTHONY, J.K., JATANA, G.S., VASA, N.J., SRIDHARRAJA, V.L.N. & LAXMIPRASAD, A.S. (2010). Modeling of laser induced breakdown spectroscopy for very low pressure breakdown conditions. *Appl. Phys. A* **101**, 161–165.

BRUGGEMAN, P., SCHRAM, D., ÁGONZÁLEZ, M., REGO, R., KONG, M.G. & LEYS, C. (2009). Characterization of a direct dc-excited discharge in water by optical emission spectroscopy. *Plasma Sour. Sci. Technol.* **18**, 025017.

COOKE, C.M. (1982). Surface flashover of gas/ solid interfaces. *Proc. of the Third International Symposium on Gaseous Dielectrics*, 337–348.

HARILAL, S.S., BINDHU, C.V., ISSAC, R.C., NAM POO RI, V.P.N. & VALLABHANAC, P.G. (1997). Electron density and temperature measurements in a laser produced carbon plasma. *J. Appl. Phys.* **82**, 5043302.

HORST, R.M.V., VERREYCKEN, T., VAN VELDHUIZEN, E.M. & BRUGGEMAN, P.J. (2012). Time-resolved optical emission spectroscopy of nanosecond pulsed discharges in atmospheric-pressure N$_2$ and N$_2$/H$_2$O mixtures *J. Phys. D: Appl. Phys.* **45**, 345201.

KENNEDY, J.T. (1995). Study of the avalanche to streamer transition in insulating gases. Ph.D. thesis. Eindhoven University of Technology, Eindhoven, The Netherlands.

KOLPAKOVÁ, A., KUDRNA, P. & TICHÝ, M. (2011). Study of plasma system by OES (optical emission spectroscopy). *Proc. of 20th Annual Conference of Doctoral Students*, **2**, 180–185.

KRILE, J.T., NEUBER, A.A. & KROMPHOLZ, H.G. (2008). Effects of UV illumination on surface flashover under pulsed excitation. *IEEE Trans. Plasma Sci.* **36**, 332–340.

KRILE, J.T., NEUBER, A.A., DICKENS, J.C. & KROMPHOLZ, H.G. (2005). Imaging of dielectric surface flashover in atmospheric conditions. *IEEE Trans. Plasma Sci.* **33**, 270–271.

KRILE, J.T., NEUBER, A.A., DICKENS, J.C. & KROMPHOLZ, H.G. (2004). DC flashover of a dielectric surface in atmospheric conditions. *IEEE Trans. Plasma Sci.* **32**, 1828–1834.

KUMAR, A., SINGH, R.K., PRAHLAD, V. & JOSHI, H.C. (2010). Effect of magnetic field on the expansion dynamics of laser-blow-off generated plasma plume: Role of atomic processes. *Laser Part. Beams* **28**, 121–127.

KUMAR, D.D.P., MITRA, S., SENTHIL, K., SHARMA, A., NAGESH, K.V., SINGH, S.K., MONDAL, J., ROY, A. & CHAKRAVARTHY, D.P. (2007). Characterization and analysis of a pulse power system based on Marx generator and Blumlein. *Rev. Sci. Instrum.* **78**, 115107/1–4.

LAGHARI, J.R. (1985). Spacer flashover in compressed gases. *IEEE Trans. Electr. Insul.* **20**, 83–92.

LAITY, G., NEUBER, A., FIERRO, A., DICKENS, J. & HATFIELD, L. (2011). Phenomenology of streamer propagation during pulsed dielectric surface flashover. *IEEE Trans. Dielect. Elect. Insul.* **18**, 946–953

LI, S.Y., THEOPHILUS, G.D. & SRIVASTAVA, K.D. (1995a). Nanosecond streak photography of discharges on spacer surface in gases. *IEEE Trans. Electr. Insul.* **2**, 114–120.

LI, S.Y., THEOPHILUS, G.D. & SRIVASTAVA, K.D. (1995b). Early stages of discharge development on insulating spacers in gases — A photographic study. *IEEE 5th International Conference on Conduction and Breakdown in Solid Dielectrics*, 361–365.

LOFHTUS, A. & KRUPENIE, P.H. (1977). The spectrum of molecular nitrogen. *J. Phys. Chem. Ref. Data.* **6**, 113–307.

MORALES, K.P., KRILE, J.T., NEUBER, A.A. & KROMP HOLZ, H.G. (2006). Pulsed dielectric surface flashover in nitrogen at atmospheric conditions. *IEEE Trans. Dielect. Elect. Insul.* **13**, 803–809

MORALES, K.P., KRILE, J.T., NEUBER, A.A. & KROMP HOLZ, H.G. (2007). Dielectric surface flashover at atmospheric conditions with unipolar pulsed voltage excitation. *IEEE Trans. Plasma Sci.* **36**, 774–782.

NEKAHI, A. & FARZANEH, M. (2011a). Rotational temperature measurement of an arc formed over an ice surface. *IEEE Trans. Dielect. Elect. Insul.* **18**, 755–759.

NEKAHI, A. & FARZANEH, M. (2011b). Excitation temperature determination of an arc formed over an ice surface using optical emission spectroscopy *IEEE Trans. Dielect. Elect. Insul.* **18**, 1829–1834.

NEKAHI, A., FAROKHI, S., FARZANEH, M. & STEWART, B.G. (2014). Arc energy and temperature during its propagation over ice-covered surfaces. *IEEE Trans. Plasma Sci.* **42**, 114–119.

PFEIFFER, W. (1982). Gas breakdown in case of steep-fronted pulses and insulator interfaces. *IEEE Trans. Dielect. Elect. Insul.* **EI–17**, 505–511.

PFEIFFER, W. & VOLKER, P. (1980). Influence of conductive particles on the dc voltage strength of spacers in compressed SF$_6$. *Proc. of the Second International Symposium on Gaseous Dielectrics*, 243–249.

RALCHENKO, Y., KRAMIDA, A.E., READER, J. & TEAM, N.A. (2013). NIST Atomic Spectra Database (ver. 5.1). http://physics.nist.gov/asd.

RAN, H., WANG, J., WANG, T., ZHANG, C., YAN, P. & WANG, L. (2013). Spacer flashover characteristics in SF_6 under repetitive nanosecond pulses. *IEEE Trans. Dielect. Elect. Insul.* **20**, 1161–1167.

ROY, A., MENON, R., MITRA, S., KUMAR, D.D.P., KUMAR, S., SHARMA, A., MITTAL, K.C., NAGESH, K.V. & CHAKRAVARTHY, D.P. (2008). Intense relativistic electron beam generation and prepulse effect in high power cylindrical diode. *J. Appl. Phys.* **103**, 014905.

SAJI, K.J., JOSHY, N.V. & JAYARAJ, M.K. (2006). Optical emission spectroscopic studies on laser ablated zinc oxide plasma. *J. Appl. Phys.* **100**, 043302.

SALIK, M., HANIF, M., WANG, J. & ZHANG, X.Q. (2014). Spectroscopic characterization of laser-ablated manganese sulfate plasma. *Laser Part. Beams* **32**, 137–144.

SHARMA, A., MITRA, S., SENTHIL, K., SHARMA, V., SINGH, S., TEWARI, S.V. & MITTAL, K.C. (2014). Energy balance aspect in KALI-30 GW high-voltage pulse power source. *Laser Part. Beams* doi:10.1017/S0263034614000470.

SUDARSHAN, T.S. & DOUGAL, R.A. (1986). Mechanisms of surface flashover along solid dielectrics in compressed gases: a review. *IEEE Trans. Electr. Insul.* **EI–21**, 727–746.

THAREJA, R.K., Abhilasha & DWIVEDI, R.K. (1995). Optical emission spectroscopy of laser-produced carbon plasma at moderate and low irradiance in an ambient atmosphere. *Laser Part. Beams* **13**, 481–492.

UNNIKRISHNAN, V.K., ALTI, K., KARTHA, V.B., SANTHOSH, C., GUPTA, G.P. & SURI, B.M. (2010). Measurements of plasma temperature and electron density in laser-induced copper plasma by time-resolved spectroscopy of neutral atom and ion emissions. *Pramana J. Phys.* **74**, 983–993.

VERHAART, H.F.A. (1982). Avalanches in insulating gases. Ph.D. thesis. Eindhoven University of Technology. Eindhoven, The Netherlands.

WEN, C. (1989). Time-Resolved Swarm Studies in Gases with Emphasis on Electron Detachment and Ion Conversion. Ph.D. thesis. Eindhoven University of Technology. Eindhoven, The Netherlands.

YAN, P., SHAO, T., WANG, J., GAO, W., YUAN, W., PAN, R., ZHANG, S. & SUN, G. (2011). Experimental investigation of surface flashover in vacuum using nanosecond pulses. *IEEE Trans. Dielect. Elect. Insul.* **14**, 634–642.

YATOM, S., STAMBULCHIK, E., VEKSELMAN, V. & KRASIK, YA.E. (2013). Spectroscopic study of plasma evolution in runaway nanosecond atmospheric-pressure He discharges. *Phys. Rev. E* **88**, 013017.